

ISTITUTO NAZIONALE DI FISICA NUCLEARE
Laboratori Nazionali di Frascati

LNF-84/32

G.Pancheri and C.Rubbia: EVENTS OF VERY HIGH ENERGY
DENSITY AT THE CERN SppS COLLIDER

Estratto da:
Nuclear Phys. A418, 117c (1984)

EVENTS OF VERY HIGH ENERGY DENSITY AT THE CERN $\overline{\text{SppS}}$ COLLIDER

G. Pancheri
INFN - Laboratori Nazionali di Frascati, P.O.Box 13 - Frascati (Italy)
and
C. Rubbia
CERN, 1211 Geneva (Switzerland)

Some general features of hadron-hadron collisions observed at the CERN $\overline{\text{SppS}}$ collider at $\sqrt{s}=540$ GeV are discussed. Transverse energy flow and multiplicity distributions accompanying jet production, as well as W and Z₀ production, are compared with minimum bias events. We examine the experimental evidence, coming from the CERN $\overline{\text{SppS}}$ collider, relevant to a possible phase transition from the hadron gas to the quark gluon plasma. Current interpretations of the anomalous behaviour observed in the multiplicity and transverse momentum spectra are discussed. The conclusion is that there are new experimental facts which favour an explanation in terms of abundance of jets in the high multiplicity region.

1. INTRODUCTION

At present, the $\overline{\text{SppS}}$ collider is the only accelerator facility which can provide enough energy to have access to the domain in which nucleus-nucleus collisions may lead to quark matter formation.

Although these are unfortunately only nucleon-(anti)-nucleon collisions, they have potentially interesting features, worth discussing at this Conference since:

- i) They give some insight into the general features of high energy collisions and some guideline on which backgrounds might affect observation of nucleus-related events.
- ii) They may provide some precursory evidence to the existence of quark-gluon plasma.

Collider results are different from what we have already seen with lower energy events for two main reasons: the dominance of jets and the production of very large multiplicities^{1,2,3}. Jets appear as the dominant, new phenomenon at the $\overline{\text{SppS}}$ Collider, thus confirming the earlier cosmic ray observations and predictions of QCD. Experimentally, large jets separate easily from debris of spectators. The other very important feature is related to the multiplicities. One finds that at $\sqrt{s}=540$ GeV, the multiplicities have risen considerably from

lower energy configurations. Since we now have $\langle N_{\text{ch}} \rangle \approx 28$, it is not uncommon to find as many as ~ 100 charged particles in the final state.

In Sect. 2, we present some experimental results related to jet production like transverse energy flow and multiplicity, while in Sect. 3 we discuss the hadronic properties of events accompanying W and Z_0 production. In sect. 4 we discuss two anomalous effects observed at the collider to see whether they can be interpreted as signals for a phase transition. In Sects. 5 and 6, various phenomenological and theoretical interpretations of these effects are examined. Recent suggestions and conclusions are presented in Sects. 7 and 8.

2. SOME GENERAL FEATURES OF JET EVENTS AT THE COLLIDER

Jets at the collider are detected through the observation of large amounts of transverse energy deposition in the calorimeters. Experimentally, this is accomplished through the use of energy flow devices, namely calorimeters which tell us simply how much energy goes where. The variable transverse energy is defined as

$$E_T = \sum E_i \sin \theta_i$$

where E_i is the energy deposited in the i th calorimeter cell and θ_i is the angle which identifies the cell position with respect to the beam as shown in Fig. 1. The energy flow technique is very powerful since:

- i) it allows to study very high multiplicity events, as it will be, for instance, the case for nucleus-nucleus collisions;
- and
- ii) it bypasses the details of quark and gluon fragmentation, and other similar final state effects, thus concentrating on the kinematics of the primary process at the parton level.

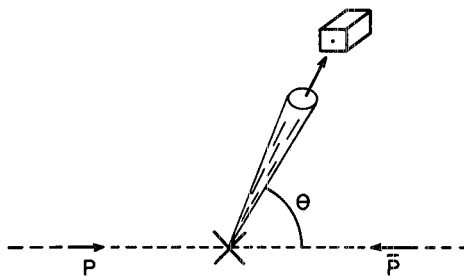


FIGURE 1
Schematic description of measurement of total transverse energy E_T

There is a direct correlation between transverse energy E_T and the multiplicity¹. If one plots the average transverse energy as a function of multiplicity one finds an almost linear growth of $\langle E_T \rangle$ with n_{ch} , as we show in Fig. 2a. Indeed, one can, approximately, write

$$\langle E_T \rangle = n_{ch} \times (1 \text{ GeV})$$

It is however important to notice that E_T grows faster than n_{ch} . This can be seen from Fig. 2b, where the mean transverse energy per particle is plotted versus the observed charged multiplicity. One finds a rise of this quantity analogous to the one reported by UA1 in the transverse momentum spectra³ and which will be discussed in detail in Sects. 4 and 6.

At sufficiently high E_T , the energy flow triggers lead to an essentially 100% sample of jet events, rather than high multiplicities. It is a striking difference from lower energies where exactly the opposite had occurred. This is indicated in Fig. 3 where the fraction of total transverse energy carried by one and two largest clusters is seen to rise to the ideal value characterizing a two jet events, i.e.

$$\text{largest } E_T \rightarrow 0.5$$

and

$$\text{two largest } E_T \text{ clusters} \rightarrow 1.0$$

The calorimeter technique gives very detailed information about the multiplicity and transverse energy flow around and within the jet. One can study the mean transverse energy per rapidity interval around the jet axis, or the mean transverse momentum, or the density of charged tracks, thus gathering important information on the particle flow. These plots, not only give a pictorial representation of the p_t and E_T distribution of the particles within the jet, but

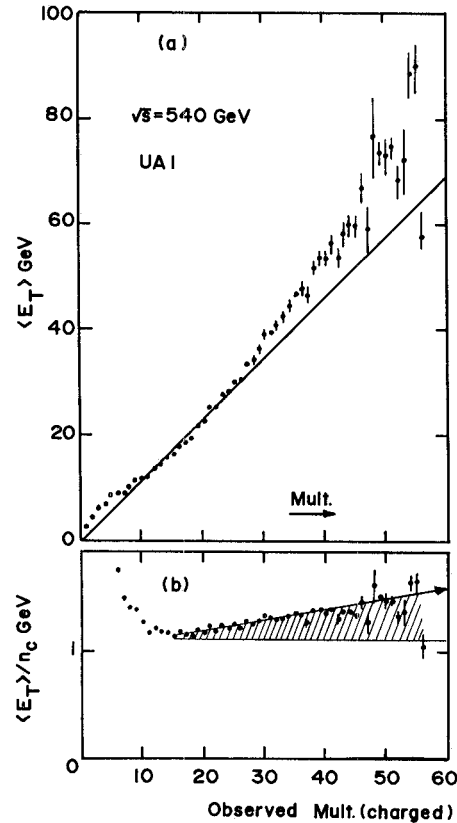


FIGURE 2
Average total transverse energy and transverse energy per particle vs charged multiplicity. The dashed region illustrates the non linear growth of $\langle E_T \rangle$ with multiplicity. UA1 data.

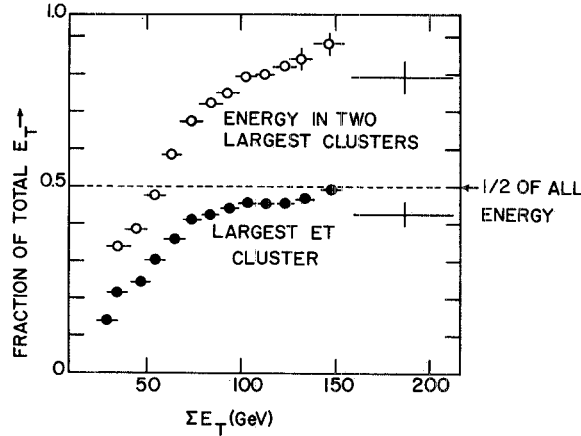


FIGURE 3
 Fraction of total transverse energy E_T carried by the largest cluster and by the two largest clusters. UA1 data.

also reveal a very important characteristic of jet events: the presence of a jet floor with an associated multiplicity larger than the one observed for the minimum bias events. In Fig. 4 we reproduce one of the multiplicity plots, comparing it with the results of two different analyses. It is important to notice that this constant, higher multiplicity background is independent of the energy of the trigger jet, i.e. of the spectator energy threshold. This appears if one plots the height of the plateau, 'off the jet' multiplicity, as a function of the spectator jet energy as in Fig. 5.

The structure associated with a given jet can be studied by separating the two jet events from those with more than two jets. The fraction of events with more than two jets is $\simeq 0.1 \pm 0.2$ of all the events with at least one jet with $E_T > 15$ GeV. We show this distribution in Fig. 6. The presence of a third jet strongly suggests the presence of a gluon bremsstrahlung mechanism, roughly α_s times smaller, and similar to the one observed in e^+e^- final state jets. It is also possible to observe the emergence of multijet states. In Fig. 7, we show a clear 4-jet event. In this figure, the large associated 'off jet' multiplicity is also visible.

The complexity of the picture we have so far discussed reflects the underlying complexity of the QCD subprocesses which lead to the production of a jet event. We shall now examine the hadronic properties of W and Z events, for which no colour adjustment is needed, and which should therefore be much more similar to the minimum bias events. The validity of this description will be discussed from the experimental point of view in the next section.

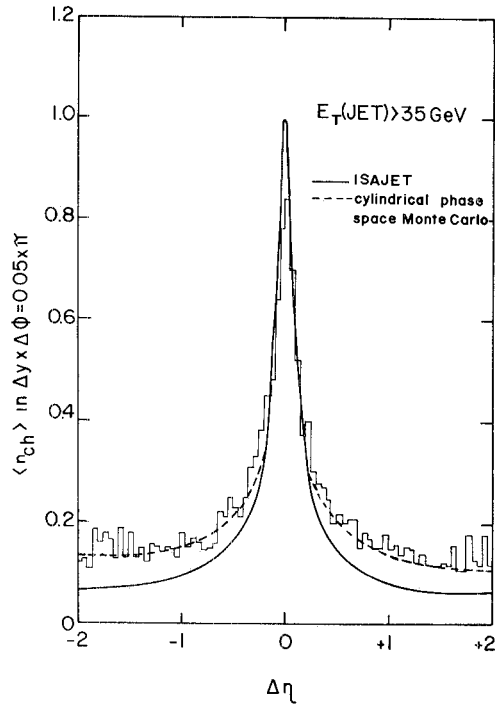


FIGURE 4

Mean charged multiplicity (in $\Delta y \Delta \phi = 0.05$) for jet events, as a function of the pseudo-rapidity interval around the jet axis. UA1 Collaboration.

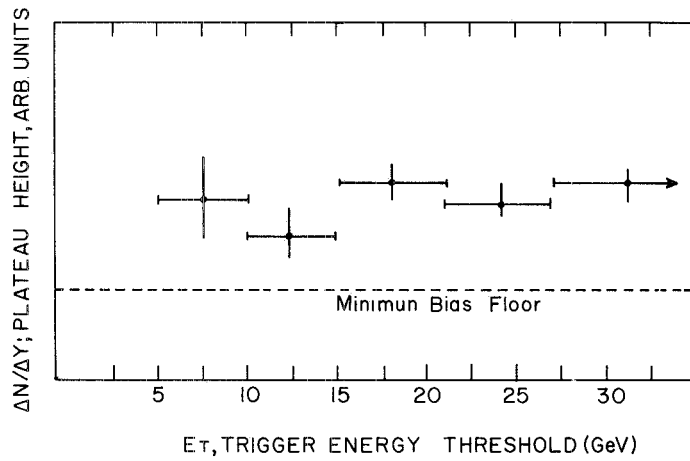


FIGURE 5

Particle density $\Delta n / \Delta y$ off the jet for different energies of the trigger jet. Preliminary data from the UA1 Collaboration.

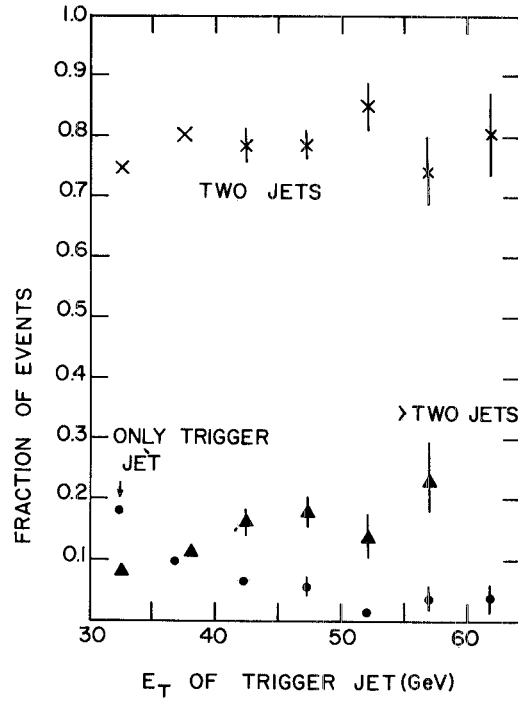


FIGURE 6
Multiplicity distribution for jets with $E_T > 15$ GeV. UA1 data.

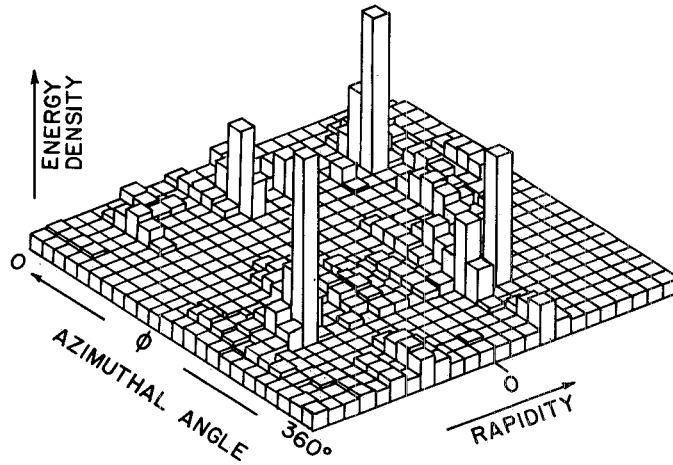


FIGURE 7
Energy flow plot for a 4 jet event. UA1 data.

3. HADRONIC PROPERTIES OF W AND Z₀ EVENTS

The detection of W and Z₀^{4,5} at the collider may well prove to be a turning point in our understanding of hadronic processes. This apparent paradox reflects the fact that through W and Z₀ production we are probing the hadronic world at a very high Q². We are, in other words, in the presence of a "poor man's" Drell-Yan! This can also be an interesting test of similar ideas on nucleus-nucleus processes.

The UA1 event sample is constituted of

$$52 W \rightarrow e\nu \text{ events} \quad 19 W \rightarrow \mu\nu \text{ events} \quad 8 Z_0 \rightarrow e^+e^- \text{ events}$$

This sample of events shows interesting features when compared to both the simple parton model and the minimum bias events. In the simple parton model, the W and Z₀ bosons should have been produced with zero transverse momentum with respect to the beam (a part from a small deviation due to the intrinsic Fermi motion) and the associated multiplicities should be the same as those for the minimum bias events. In QCD the W acquires a transverse momentum because of emission of soft and hard gluons from the initial state partons. Thus the appearance of large values of W-transverse momentum is a clear confirmation of QCD effects of the type already observed at lower energy for the Drell-Yan pairs.

The presence of a hard gluon bremsstrahlung process can be detected experimentally by selecting events where W and Z₀ are accompanied by a visible jet. The fraction of these W events is shown in Fig. 8 for a sample of 43 W → eν events. At present, there are 14 events with a jet out of a total of 52 W events. In comparison, for the Z₀, we have 6 events with a jet out of a total of 8 events.

When the jet events are taken out of the W sample, the relative distributions are in very good agreement with the expectations from the minimum bias events. We show this in Fig. 9 for the rapidity distribution and in Fig. 10 for the transverse momentum distribution of charged tracks accompanying W-production. We also show similar

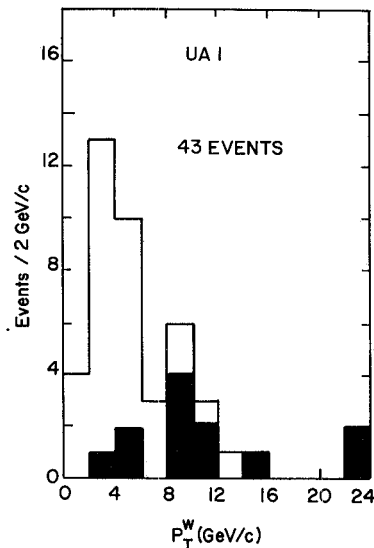


FIGURE 8
W-boson transverse momentum distribution. The shaded blocks correspond to events with a visible jet activity, i.e. $p_{T1}^{cal}(\text{jet}) > 5$ GeV/c and $E_T^{cal}(\text{jet}) > 10$ GeV. UA1 Collaboration.

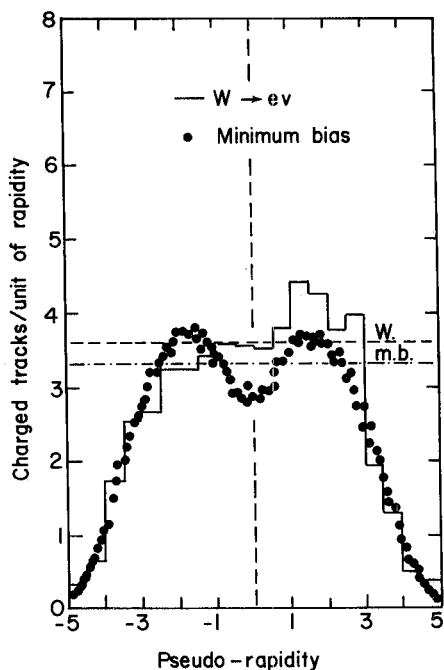


FIGURE 9
Particle density vs pseudo-rapidity for $W \rightarrow e\nu$ events. The dots refer to the minimum bias events. UA1 Collaboration.

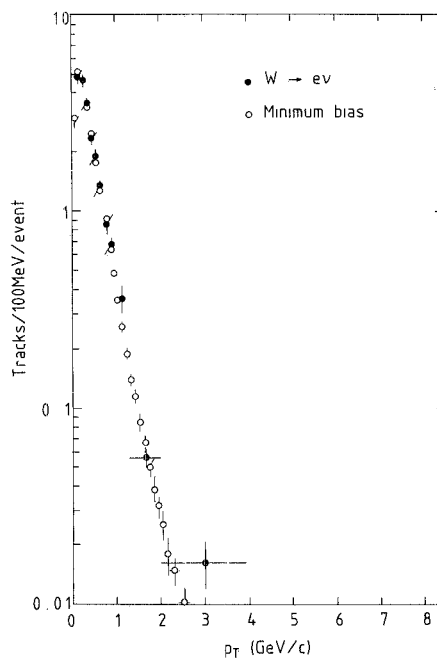


FIGURE 10
Transverse momentum distribution of charged particles accompanying W production, compared with the minimum bias events. UA1 Collaboration.

analyses for $Z_0 \rightarrow e^+e^-$. As one can see from Fig. 11, it appears that for the Z -boson the particle density in the central region is higher than for the minimum bias events. This is reflected in a flatter p_t distribution of associated charged tracks, as shown in Fig. 12.

4. ANOMALOUS MULTIPLICITY FEATURES FROM UA1 AND UA5

The formation of a quark gluon plasma is expected from QCD when the energy density and/or the temperature, measured over an extended region, are so high that the quarks are no longer confined to the typical hadronic matter dimensions of 1 fm, but freely move within the larger region. The expectation is that for sufficiently high energy density, there should be a phase transition from the hadron gas to a quark gluon plasma⁶. Such a transition has been studied and observed in lattice gauge theories^{7,8}. This transition can be studied in high

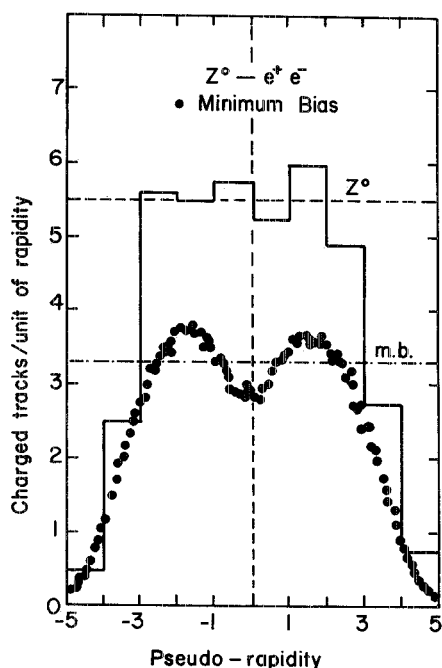


FIGURE 11
Particle density vs pseudo-rapidity for Z_0 events. The dots refer to the minimum bias events. UA1 Collaboration.

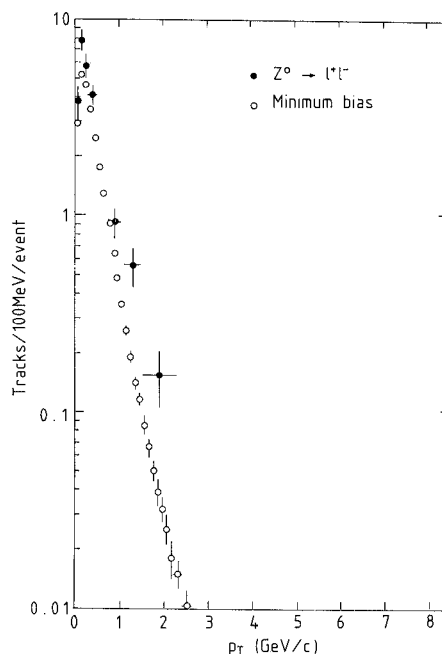


FIGURE 12
Transverse momentum of charged particles accompanying Z_0 production, compared with the minimum bias events. UA1 Collaboration.

energy collisions relating typical high energy observables like particle density and transverse spectra to thermodynamical quantities like entropy and temperature. In particular, the number of particles measures the entropy⁹ and since the typical longitudinal extent of the system is measured by the spread in rapidity¹⁰, the particle density $\Delta n/\Delta y$ appears proportional to the entropy density of the blob of hot hadronic matter produced during the collision. Moreover, correlations between the transverse momentum spectra of the secondaries produced in the central region and particle multiplicity may give information on a possible phase transition. Indeed, because of the limiting behaviour

$$e^{-p_t/\langle p_t \rangle}$$

observed at lower energies, $\langle p_t \rangle$ is a measure of the temperature of the system¹¹.

Two anomalous effects have been observed during the last year by the UA1³ and UA5¹² Collaborations. The UA1 effect, first reported at the 1982 Paris

Conference, shows a strong multiplicity dependence of the transverse momentum distribution of charged particles produced in proton-antiproton collisions at $\sqrt{s}=540$ GeV. The effect is shown in Fig. 13. This figure shows that inclusive

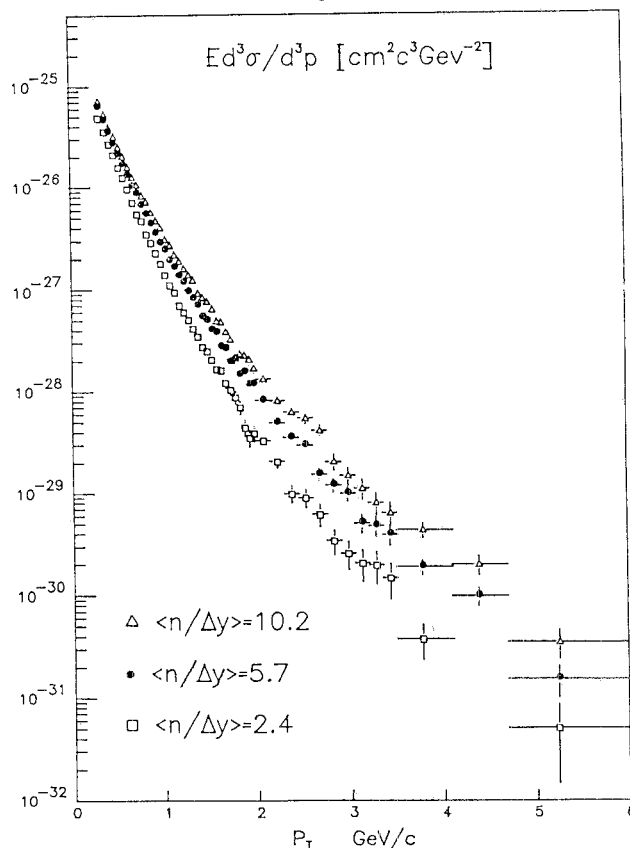


FIGURE 13

Inclusive p_t spectrum for different multiplicity densities. UAI Collaboration.

single particle spectra, when analysed in different multiplicity regions, exhibit a flattening of the cross-section with increasing multiplicity. This effect was not completely unexpected. In fact, a correlation between transverse spectra and multiplicity has been observed in cosmic ray experiments¹³. The observation of cosmic ray jets in emulsion chambers, in the region of primary energy 10 ± 1000 TeV, shows that jets are characterized by 3 distinct types of multiple pion production. In Fig. 14 we reproduce the observed γ -rays transverse momentum spectra for the three different type of jets in which one can divide the entire sample¹³. In the figure we have also indicated the characteristic number of γ per unit rapidity interval. The broadening of the p_t -distribution with increasing

multiplicity is very evident, larger in fact than the effect observed at the collider. In Table I, we reproduce, from Ref. 13), the main characteristics of these events. For a comparison with collider data, we recall that $n_\gamma = 2n_\pi = n_{ch}$ and $\langle p_t \rangle_\gamma = \frac{1}{2} \langle p_t \rangle_\pi$. The difference between events in various multiplicity intervals has been studied using the fire-ball hypothesis. To date, it is not understood how much of the effect can be attributed to interaction of complex nuclei and how much is a genuine new phenomenon. One cannot but stress however the correlation between multiplicity and transverse spread of the produced pions: higher multiplicity events are characterized by flatter p_t distributions or, at high multiplicity, pions are produced at larger angles. It is the same effect, albeit not as large, which has been observed at the collider.

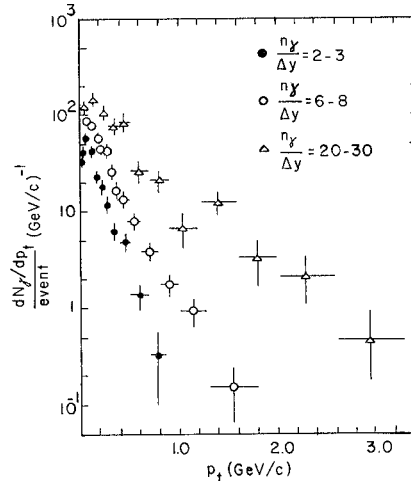


FIGURE 14
Transverse Momentum Distribution of γ -rays observed in cosmic ray events, for three types of jets; Mirim jets; açu jets; guaçu jets. (Ref. 13).

TABLE I

type of jet	characteristics of produced gamma-produced rays		composition of particles
	$\langle p_t \rangle$	n_γ per unit rapidity interval	
Mirim-jet	140 MeV/c	2-3	Mainly pions
Açu-jet	220	6-8	non-negligible
Guaçu-jet	400-500	20-30	yield of X-particles

Remark: Mirim, Açu and Guaçu mean small, large and very large in BrazilianIndian language.

After the observation of the above correlations by the UA1 Collaboration, the effect has been searched for at lower energies by other groups.

No effect was found by NA5 at $\sqrt{s}=20$ GeV¹⁴. The effect has also been searched at ISR by the ABCDHW Collaboration¹⁵. While no multiplicity dependence was detected at $\sqrt{s}=30$ GeV, a significant effect was observed at $\sqrt{s}=63$ GeV. In Figs. 15a, and 15b, we reproduce their results.

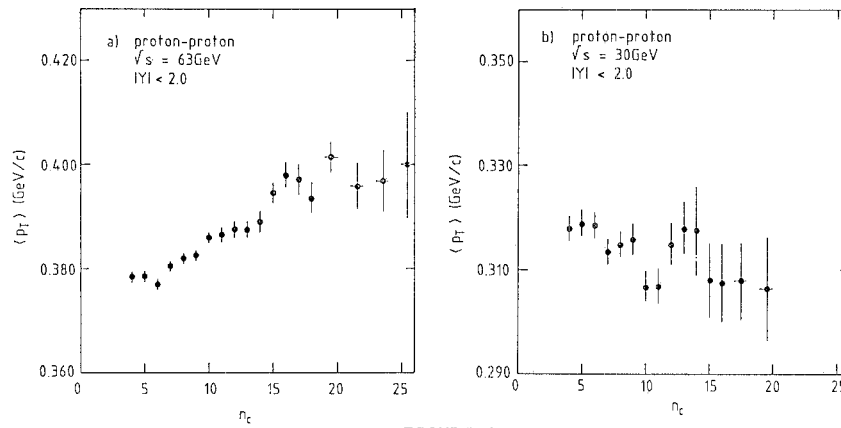


FIGURE 15
Mean charged momentum for charged particles produced in the central region of rapidity, $|y| < 2$, versus charged multiplicities at c.m. energies $\sqrt{s} = 30$ GeV and $\sqrt{s} = 63$ GeV. Ref. 15).

Although significant, the effect is however not as dramatic as at the collider, as one can see from Fig. 16, where the collider data are directly

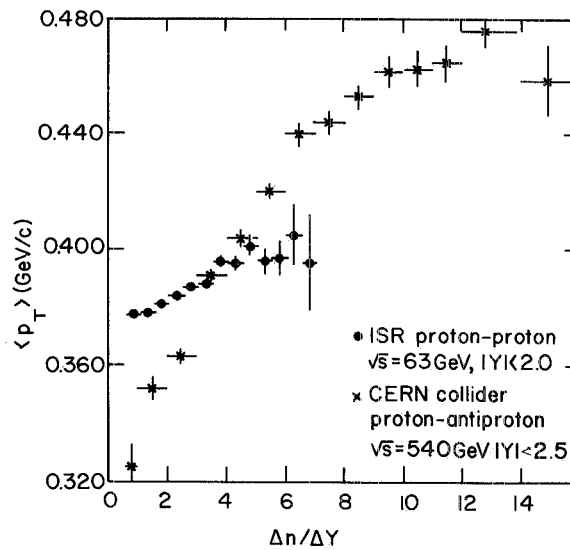


FIGURE 16
Mean transverse momentum as a function of charged particle density in the central rapidity region, at ISR and $\bar{p}p$ Collider. Ref. 15).

compared with ISR data at $\sqrt{s}=63$ GeV. From the accelerator data, we can thus conclude that some sort of threshold seems to occur in the middle of the ISR range. As the energy increases, pions in the high multiplicity region are found to be emitted, on the average, at larger angles.

The second anomalous observation at the collider concerns the high multiplicity tail of the KNO function. The UA5 Collaboration^{12,16} has reported an apparent excess of events in the multiplicity distribution for $n > 3 \langle n \rangle$. The apparent excess refers to the asymptotic KNO curve as obtained from low energy data. We recall here very briefly the main facts relative to the well known scaling property of the multiplicity distribution, known as KNO scaling. In 1968, Koba, Nielsen and Olesen¹⁷ argued, on the basis of Feynman scaling and the definition of topological cross-sections, that the function

$$\psi(n,s) = \langle n(s) \rangle \frac{\sigma_n(s)}{\sigma_{inel}(s)}$$

is independent of s and is only a function of the KNO variable $z=n/\langle n \rangle$. This scaling property has been found to be approximately true from very low energies, $\sqrt{s}=1.5$ GeV, up to ISR energies, $\sqrt{s}=63$ GeV¹⁷. In Fig. 17 we show a recent compilation of low energy data¹⁸ together with an approximate fit, drawn to guide the eye and to illustrate the scaling behaviour. When this approximate curve is compared with the UA5 data as in Fig. 18, one immediately sees the appearance of possible scaling violations. To pin point the discrepancy, one can study the fraction of events above a given multiplicity threshold at different energies. This was done by the UA5 group¹⁶ and we show it in Fig. 19 for $n > 2 \langle n \rangle$. We see that while, at lower energies, only 2% of the events are in this region, at the collider this fraction has increased by a factor 3. Clearly the source of the effect is a phenomenon which is not dominant in the overall cross-section but which may become quite important at large multiplicities. In the following section, some of the current interpretations of the effects discussed here will be examined.

5. THEORETICAL INTERPRETATIONS OF THE KNO FUNCTION

The apparent validity of KNO scaling and the shape of the multiplicity distribution have been the subject of a large number of theoretical and phenomenological interpretations. The shape has been obtained through geometrical-dynamical models^{19,20,21}, QCD clusters^{22,23}, dual parton model²⁴, QCD jet calculus²⁵⁻²⁸, generalized Bose-Einstein distributions²⁹, and soft QCD radiation³⁰. In the following, we shall try to discuss in detail some of these approaches to determine if and how they can incorporate scaling violations of

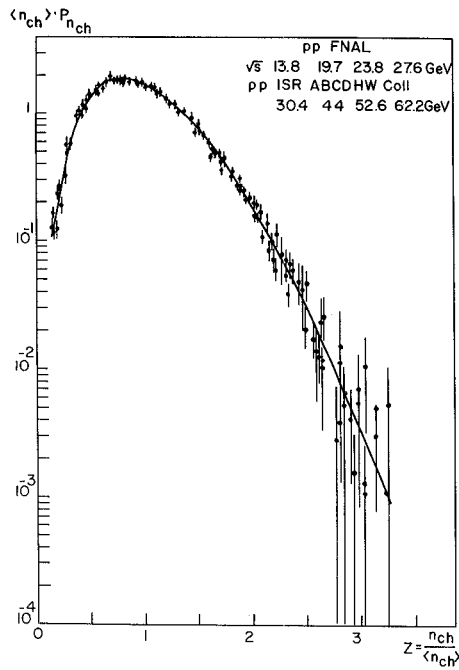


FIGURE 17
Non single diffractive multiplicity distributions from $\sqrt{s}=13.8$ GeV to $\sqrt{s}=62.2$ GeV. Refs. 17) and 18).

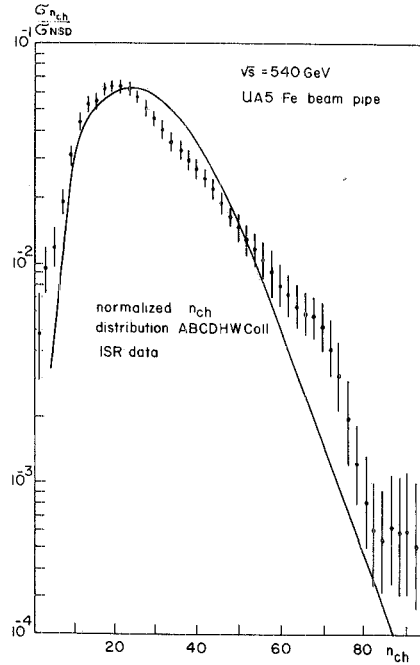


FIGURE 18
Non single diffractive multiplicity distribution at $\sqrt{s}=540$ GeV. UA5 Collaboration, Refs. 12) and 16). The curve is the approximate fit from lower energy data.

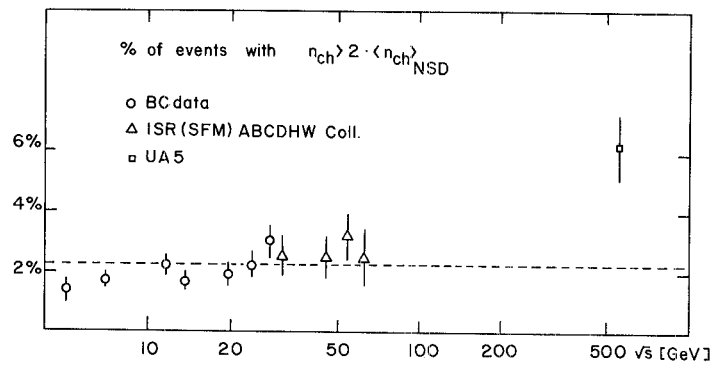


FIGURE 19
Fraction of events with charged multiplicity larger than twice the mean value. Ref. 18). Single diffraction not included.

the type observed by UA5.

In the geometrical-dynamical models, the multiplicity distribution is related to the impact parameter representation of the scattering process. These models are based on the physical idea that central collisions ($b \approx 0$) contribute to large multiplicity, while large values of the impact parameter characterize small multiplicity events. Scaling is then understood as a reflection of geometric scaling. In Ref. 21), Barshay introduces the idea of a normalized multiplicity distribution for each value of the impact parameter. The hadronic distribution is given by:

$$P_n(s) = \frac{\int P_n(b,s) \sigma_{inel}(b,s) db^2}{\int \sigma_{inel}(b,s) db^2}$$

Upon using geometric scaling for the eikonal $\Omega(b,s)$, the inelastic cross-section is parameterized as

$$\sigma_{inel}(s) = \int (1 - e^{-2\Omega}) db^2 \approx \int e^{-\lambda b^2} db^2$$

Scaling in the variable $z = n / \langle n \rangle$ is obtained since the function $P_n(b,s)$ depends upon b and s only through the variable

$$z = \frac{n}{\langle n(b,s) \rangle}$$

with

$$\langle n(b,s) \rangle = N(s) \sqrt{\Omega(b,s)}$$

The functional dependence of $P_n(b,s)$ on the variable z is taken to be same as that of the corresponding function for e^+e^- . Barshay fits well the KNO function from lower energies up to ISR values. To accommodate scaling violations, Barshay invokes a two component mechanism³¹, by adding to the main term a very narrow distribution which, at high energy, is more sensitive to small values of b (and hence to large n): the physical idea is that $\langle n(s) \rangle$ will slowly change its functional form as the new addition, a function of s , becomes more important.

Barshay asks two interesting questions:

- (i) Does the distribution for e^+e^- have a tendency to narrow or to broaden as the energy increases?
- (ii) Since $\langle n(b,s) \rangle$ for small b increases more strongly with energy than at large impact parameters, is the system at small b approaching the quark-gluon plasma phase?

KNO scaling is also obtained by summing QCD jets. Using the jet calculus technique^{25,26}, it has been possible to derive an expression which describes the

growth of the mean multiplicity from low energy up to $\sqrt{s} = 540$ GeV. This expression, which is given by^{27,28,32}

$$\langle n(s) \rangle \sim Ae^{\sqrt{B \ln s}}$$

may provide a better fit to the data than the lower energy parameterization¹⁸:

$$\langle n(s) \rangle = a + b \ln s + c (\ln s)^2$$

Chain fragmentation and dual parton models²⁴ obtain the shape of the KNO function by summing Poisson distributions with a weight given by the rapidity spectra. Kaidalov proposes an expression which shows a broadening at large multiplicity with increasing energy. Thus, in this calculation, scaling violations of the type observed by UA5, are expected.

Approximate scaling is obtained in the cluster type approach of Sterman and Hayot²³. This approach gives results similar to those obtained by exponentiating the lowest order QCD diagrams in the Leading Logarithm Approximation (LLA). This QCD calculation predicts very slow scaling violations of the type $\ln \ln(s/\Lambda^2)$. Their effect is to produce a narrower distribution as the energy increases.

Recently Carruthers and Shih²⁹ have obtained the shape of the KNO function from very general statistical laws. They propose an expression obtained from a generalized Bose-Einstein distribution:

$$P_n(k) = \frac{(n+k-1)!}{n!(k-1)!} \left[\frac{\bar{n}}{k} \right]^n \frac{1}{(1 + \frac{\bar{n}}{k})^k}$$

with k , the number of cells, which regulates the shape of the function. By altering how many cells participate to the process, the shape can be changed. To incorporate scaling violations of the type observed by UA5, one then needs to decrease the number of cells as the energy increases. This model has the attractive feature of describing KNO scaling in a very general statistical framework.

That the shape of the KNO function can be thought in very general terms, also follows from the interpretation put forward in Ref. 30). There, the shape of the distribution appears as a special (QCD) case of the expression one obtains when summing massless quanta emitted by independent semiclassical sources, with a constraint due to overall energy conservation. In the energy variable, this summation leads to the distribution

$$dP(K_0) = \frac{dK_0}{2\pi} \int dt e^{+iK_0 t} \exp\left(-\int d^3 \bar{n}(k)(1 - e^{-ikt})\right)$$

where $d^3 \bar{n}(k)$ is the spectrum of single quanta emitted by a semiclassical source. This summation procedure, when applied to QED, produces the typical soft photon

spectrum $k^{-1-\epsilon}$. The same spectrum averaged over the condensed matter coordinates, like in electrical circuits, reproduces the well known 1/f noise²⁹. The same summation technique can also be used for soft graviton emission³⁴. What discriminates among different physical processes is the energy spectrum of the single quantum which is exponentiated by the summation, i.e. the nature of the point-like current which generates the massless fields. For the hadronic case, the distribution is averaged over the hadronic matter coordinates. The KNO function is then obtained by making use of the following two hypotheses:

$$\sum_1^{n \text{ pions}} \omega_i = K_0$$

with ω_i the energy of each pion, and

$$P_n = \frac{\sigma_n}{\sigma_{inel}} = \langle \text{Resummed Soft Gluon Distribution} \rangle_{\text{Hadronic Matter}}$$

One obtains the following expression for the KNO function:

$$\begin{aligned} \psi\left(\frac{n}{\langle n \rangle}\right) &= \langle n \rangle P(n,s) = \\ &= \beta(s) \int \frac{dt}{2\pi} e^{+i\beta \frac{n}{\langle n \rangle} t - \beta \int \frac{dk}{k} (1 - e^{-ikt})} \end{aligned} \quad (1)$$

with $\beta(s) \sim \ln s$. The value $\beta(s)=1.82$ gives a very good fit to the UA1 data for $|\eta| < 3.5$. The spectrum β is proportional to the kinematical cuts, thus for $|\eta| < 1.5$ the relative data should be fitted by a smaller β . The two fits are shown in Figs. 20a and 20b.

So far this model does not show scaling violations of the kind presently discussed. In fact, in this model, as the energy increases, the KNO curve will go to zero more rapidly at large z . This behaviour can be detected if we use the approximation:

$$\psi(z) \approx \beta \frac{(\beta z)^{\beta-1}}{\Gamma(\beta)} e^{-\beta z}$$

Thus this bremsstrahlung model shows that, by summing Poisson distributions with an energy conservation constraint, one obtains scaling violations, but opposite to the type observed. However, one should not expect such a simple soft gluon model to correctly predict what happens at really large z , which, in this context, corresponds to really large energy being emitted by the colliding partons. For, at very large energy, for instance, rescattering may become important. Besides rescattering and contributions from hard scattering between the constituents, there might also be spectator interactions, which would also increase the multiplicity.

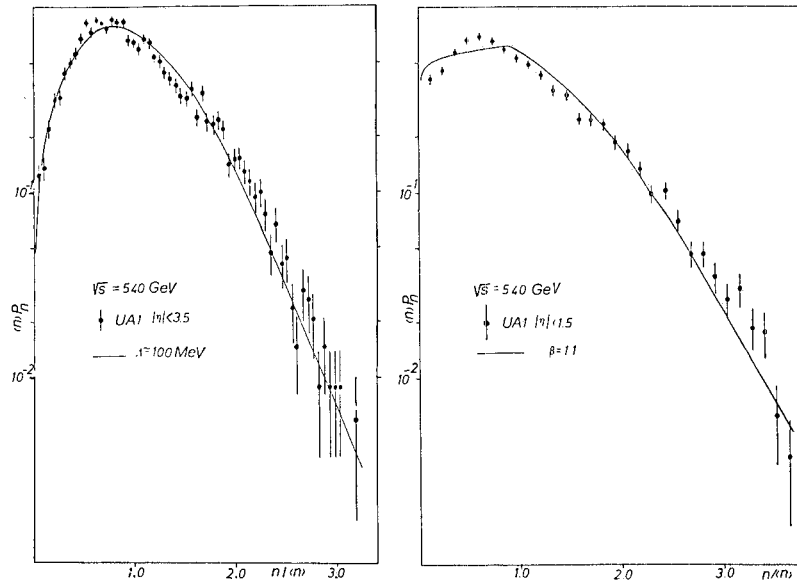


FIGURE 20

UA1 Multiplicity distribution at $\sqrt{s}=540$ GeV. Data are from Ref. 1). The solid line is the soft gluon formula from Eq. (1) of the text.

6. PHENOMENOLOGICAL AND THEORETICAL INTERPRETATIONS OF THE UA1 EFFECT

The most interesting discussion of the UA1 effect is due to L. Van Hove³⁵ who has discussed it as a possible signal of a phase transition from the hadron gas to the quark-gluon plasma. Following the hydrodynamical model, he notices that while the particle density dn/dy reflects the entropy, the transverse momentum of the inclusively produced particles receives contributions from both the temperature and the transverse expansion of the system. The latter consists originally of a blob of hot hadronic matter formed in the collision between very high energy hadrons.

Thus, at the beginning the entropy increases as the temperature, and hence $\langle p_t \rangle$, increases. If there is phase transition, however, the temperature will remain constant while the entropy increases through the transition. After the quark-gluon plasma has formed, the temperature should start increasing again for growing n , but this will not reflect in a similar $\langle p_t \rangle$ increase since the outgoing pions have been produced when the quarks and gluons froze into hadrons, at a lower temperature. This mechanism thus explains the apparent

saturation of the p_t -spectra at very large n . The growth of $\langle p_t \rangle$ with multiplicity appears because both the temperature and the entropy of the system are increasing towards the transition point, while the saturation is understood because the pions will always appear at the temperature at which they have been produced, i.e. around the critical temperature. In Fig. (21), we reproduce the expected $\langle p_t \rangle$ vs. dn/dy dependence. This qualitative behaviour is very similar to the one observed in the UA1 effect.

On the phenomenological level, there exists a more standard interpretation by S. Barshay³⁶. As mentioned in relation to the UA5 effect, Barshay introduces a normalized multiplicity distribution in the impact parameter space. With this distribution, more particles are produced at small values of the impact parameter than otherwise. Thus n is large for central collisions. Barshay calculates the average value of the squared impact parameter for each multiplicity value, $\langle b^2(n,s) \rangle$ and relates it to the transverse spectra through a functional relationship of the type

$$\langle p_t(n,s) \rangle \approx \langle b^2(n,s) \rangle^{-\gamma}$$

where γ is different at different energies. The choice of γ is, at present, phenomenological. It should be noticed that, in Barshay's model, the mean transverse momentum as a function of n does not show complete saturation, but only a slowing down of the rate at which it grows.

An interpretation which differs from both of the above, but which may lead to understand both the UA1 and the UA5 effect, has been put forward by M. Jacob³⁷. Jacob suggests that the collider energy is high enough for a new type of reaction mechanism to occur. Just like it was the case for acv events in cosmic ray observations, it is possible that, from ISR to the collider, an energy threshold has been crossed such that many low- x partons have now enough energy to undergo hard scattering and produce several mini-jets, of a few GeV each, which fragment independently from one another. This produces both an increase in the particle density as well as an increase in the average $\langle p_t \rangle$, since the jet mechanism

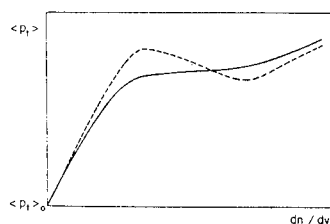


FIGURE 21
Expected structure in the p_t versus dn/dy correlation resulting from a possible phase transition. Reproduced from Ref. 35).

allows for large angle scattering. The threshold effect would then be due to the same mechanism which is responsible for the emergence of jets from lower energy configurations.

7. SUGGESTIONS FROM RECENT EXPERIMENTAL OBSERVATIONS

It is by now apparent that we are witnessing two anomalous behaviours, relative to lower energy data, which both involve large multiplicity effects. A study of the UA1 data as presented in Sect. 2 suggests the following:

(i) Events with jets show a remarkable increase of particle multiplicity away from the trigger jet. This can be seen from Fig. 4 where the mean charged multiplicity per unit of rapidity and azimuthal interval, in the presence of a jet, is plotted for different rapidity intervals, centered around the jet axis. Away from the jet, one notices a rather constant "jet floor", which can be called the jet associated multiplicity. This jet associated multiplicity appears to be more than twice the multiplicity of the minimum bias events. This constant, higher multiplicity background, can be explained as due to the presence of additional small jets.

(ii) Mini-jets or low energy jets can easily go undetected since present detection thresholds for jet algorithms are high. We could of course argue that mini-jets need not have the same associated high multiplicity as regular jets. A study of associated multiplicities as a function of the trigger jet energy threshold, as in Fig. 5, shows them to be rather constant even for low E_T values. We can therefore expect these high multiplicities to persist also for those undetected jets.

It may very well be that, selecting events at high multiplicity, lead to contamination from broad undetectable jets and thus to an increase of the observed p_t . At the same time, the jet and mini-jet mechanism can also be responsible for the increase at large multiplicities observed in the KNO function, since this is a mechanism which was not present at lower energies and which is becoming increasingly important at high energy. This might explain the observed KNO scaling violations.

8. CONCLUSIONS

Present data from the CERN Collider, of interest to quark-matter formation, have been discussed. It appears that the anomalous high multiplicity tail observed by the UA5 Collaboration and the multiplicity dependence of inclusive p_t

spectra reported by UA1 can probably be explained by invoking the persistent high multiplicity associated with low energy (few GeV) jet events. These events are certainly present and their effects are sufficiently important at collider energy as to mask possible quark-matter formation a la Van Hove.

REFERENCES

- 1) G. Arnison et al., Phys. Letters 107B, 320 (1981); 123B, 108 and 115 (1983). UA1 Collaboration.
- 2) M. Banner et al., Phys. Letters 115B, 59; 118B, 203 (1982). UA2 Collaboration
- 3) G. Arnison et al., Phys. Letters 118B, 167 (1982). UA1 Collaboration.
- 4) G. Arnison et al., Phys. Letters 122B, 103 (1983); Phys. Letters 126B, 398 (1983). UA1 Collaboration.
- 5) M. Banner et al., Phys. Letters 122B, 476 (1983); P. Bagnaia et al., Phys. Letters 129B, 130 (1983). UA2 Collaboration.
- 6) For a review: G. Baym, Quark Matter Formation and Heavy Ion Collisions (Bielefeld, 1982), Ed. by M. Jacob and H. Satz, World Scientific Pub. (1982).
- 7) L.D. McLerran and B. Svetitsky, Phys. Letters 98B, 195 (1981); J. Kuti, J. Polonyi and K. Szlachany, Phys. Letters 98B, 199 (1981). K.Kajantie, C. Montonen and E. Pietarinen, Z. Phys. C9, 253 (1981).
- 8) J. Engels, F. Karsch, I. Montvay and H. Satz, Phys. Letters 101B, 89 (1981); Nuclear Phys. B205, (FS5), 545 (1982); I. Montvay and E. Pietarinen, Phys. Letters 115B, 151 (1982).
- 9) H. Satz, Lectures given at the Intern. Summer Institute in Theoretical Particle Physics, Hamburg 1975. Proc. published as Current Induced Reactions, J.G. Korner, G. Kramer and D. Schilknecht editors. Springer Verlag (Berlin 1976).
- 10) J.D. Bjorken, Lecture given at the Intern. Summer Institute in Theoretical Particle Physics (Hamburg 1975). Proc. published as Current Induced Reactions, J.G. Korner, G. Kramer and D. Schilknecht (Springer Verlag, Berlin, 1976).
- 11) R. Hagedorn, Cargese Lectures 1971, Ed. Schatzman, Gordon and Breach (New York, 1973).
- 12) K. Alpgard et al. Phys. Letters 121B, 209 (1983). UA5 Collaboration.
- 13) C.M.G. Lattes et al., Phys. Rep. 65, 151 (1980).
- 14) G. Matthiae, Rapporteur's Talk at the European High Energy Physics Conference, (Brighton, UK, July 1983).
- 15) A. Breakstone et al., Contributed Paper 216, European High Energy Physics Conference (Brighton, UK, July 1983).
- 16) P. Bockman; Como Conference, (August 1983).
- 17) Z. Koba, H.B. Nielsen and P. Olesen, Nuclear Physics B40, 317 (1972).
- 18) W. Thome et al., Nuclear Physics B129, 365 (1977).
- 19) C.S. Lam and P.S. Yeung, Mc Gill University Preprint, (1982).
- 20) T.T. Chou and C.N. Yang, Phys. Letters 116B, 301 (1982).
- 21) S. Barshay, Phys. Rev. Letters 22, 1609 (1982); Phys. Letters 116B, 193 (1982).

- 22) E.H. Ge Groot, Phys. Letters 57B, 159 (1975).
- 23) F. Hayot and G. Sterman, Phys. Letters 121B, 419 (1983).
- 24) A.B. Kaidalov and K.A. Ter-Martirosyan, Phys. Letters 117B, 247 (1982).
- 25) D. Amati and G. Veneziano, Phys. Letters 83B, 87 (1979).
- 26) A. Bassetto, M. Ciafaloni and G. Marchesini, Phys. Letters 83B, 207 (1979); Nuclear Phys. B163, 477 (1980).
- 27) W. Furmanski, R. Petronzio and S. Pokorski, Nuclear Phys. B155, 253 (1979).
- 28) K. Konishi, Rutherford Preprint RL 79-035 (1979).
- 29) P. Carruthers and C.C. Shih, Phys. Letters 127B, 242 (1983).
- 30) G. Pancheri and Y.N. Srivastava, Phys. Letters 128B, 433 (1982).
- 31) S. Barshay, "A Formula for Violation of the Scaling Behaviour in Multiplicity Distributions at the CERN Collider", Aachen Preprint (October 1983).
- 32) Yu.L. Dokshitzer, V.S. Fadin and V.A. Khoze, Z. fur Phys. C18, 37 (1983).
- 33) A. Widom et al., Physical Rev. B26, 1475 (1982); Phys. Rev. B27, 3412 (1983).
- 34) Y.N. Srivastava, Lectures on Radiation and Noise in "Stochastic Processes Applied to Physics and Other Related Fields", World Scientific (1983).
- 35) L. Van Hove, Phys. Letters 118B, 138 (1982).
- 36) S. Barshay, Phys. Letters 127B, 129 (1983).
- 37) M. Jacob, Cern Th-3693. To be published in the Proc. of SLAC Topical Conf. (27-29 July 1983).